ARCHIVES OF ACOUSTICS
25, 4, 395–422 (2000)

ADAPTATION OF IMAGE RECONSTRUCTION ALGORITHM FOR PURPOSES OF ULTRASOUND TRANSMISSION TOMOGRAPHY (UTT)

A.B. DOBRUCKI and K.J. OPIELIŃSKI

Wrocław University of Technology
Institute of Telecommunication and Acoustics
(50-370 Wrocław, Wybrzeże Wyspiańskiego 27, Poland)
e-mail: ado@zakus.ita.pwr.wroc.pl, popi@zakus.ita.pwr.wroc.pl

In this research, the convolution and backprojection method has been adapted for the purposes of image reconstruction in ultrasound transmission tomography (UTT). In particular, a complete computer algorithm enabling the use of different convolving and interpolation functions has been developed. A technique of reducing and scaling the tomographic measuring data to minimize the reconstruction errors is proposed. The convolution and backprojection method was optimized through a choice of a versatile convolving function and a simple interpolation function, and it was tested using simulated and actual tomographic measuring data. After reconstruction, good-quality images were obtained. It has been found that the number of measuring rays determines the resolution of an image, the accuracy with which the size of structures is imaged and the accuracy with which the image point values are reconstructed, whereas the number of measuring projections determines the dynamics and distortion of an image. Because of computation time and image blur, an optimum reconstruction grid size, according to the visualization quality criterion, should be chosen. The convolution and backprojection algorithm optimized in this research can be applied directly to the UTT visualization of the internal structure of objects as a distribution of local sound velocities in this structure, reconstructed on the basis of measurements of mean times of the passage of an ultrasonic wave through a cross-section of an object immersed in water, in a parallel ray projection geometry.

1. Introduction

In ultrasound transmission tomography (UTT) measurements in a parallel ray projection geometry, ultrasonic transducers: the sending one and the receiving one, are positioned opposite each other with the investigated object inbetween (1st generation of measuring data acquisition) [13]. A packet of measurements is obtained while moving the two transducers over distance s and rotating them at the same time by angle ψ along and around the object (Fig. 1). The measuring cycle ends after a rotation by an angle of 180°. Each shift of the transducers is called a ray and each rotation of them — a projection. A result of the measurement is a set of mean values of a certain acoustic parameter in the measured cross-section of an object for M rays and N projections. The values constitute basic data for the image reconstruction.

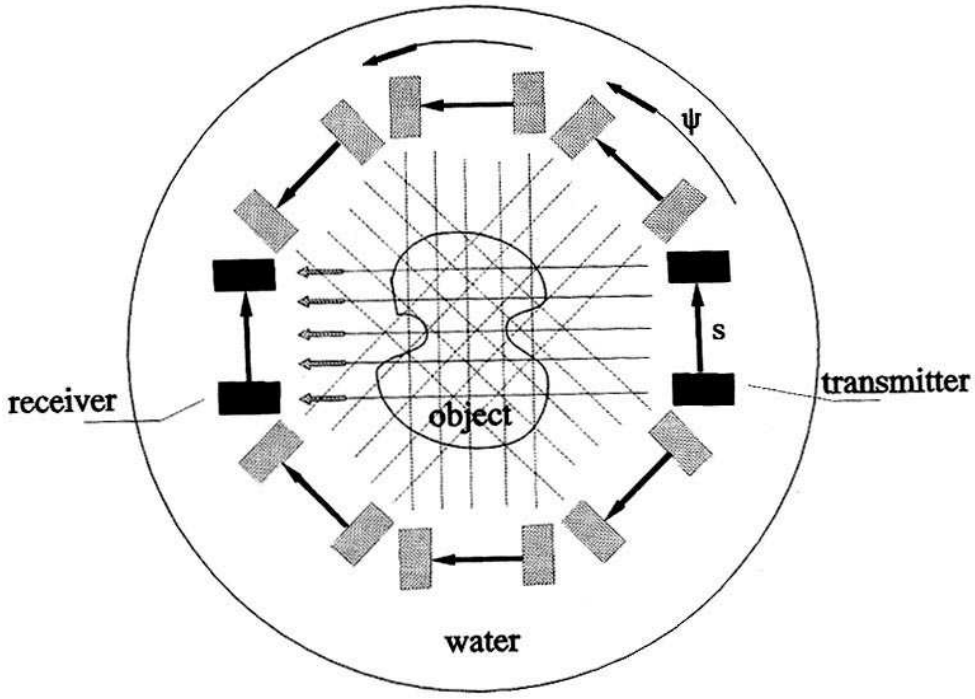

Fig. 1. Technique of measurement in UTT by means of parallel ray projection method.

An image reconstruction algorithm provides a mathematical basis for tomography. To visualize the internal structures of objects one must be absolutely certain that image reconstruction from the measuring data is correct. Therefore it is highly important that a proper reconstruction algorithm is selected, adapted to the particular measuring data, optimized and tested. These operations make it possible to detect and minimize any calculation errors which, compounded by measuring errors included in the tomographic data, could distort the reconstructed image even more.

In the present research, an image reconstruction algorithm was selected and made suitable for entering of the measuring data in the form of ultrasonic wave propagation mean velocities in a parallel ray projection geometry. Then the algorithm was optimized to minimize the calculation errors, tested and implemented as a computer program.

2. Choice of algorithm

An important problem in UTT, requiring a thorough survey of the existing reconstruction methods, is the choice of an image reconstruction algorithm. First, one must choose from the two types of algorithms: the transform method [6] or the finite series-expansion reconstruction method [1], considering their advantages and disadvantages. The first computer-assisted X-ray tomograph, invented by Hounsfield and produced by EMI, used the algebraic reconstruction technique (ART) [1] and the expansion- into-series

concept, whereas the present commercially available tomographs for medical applications do not use the series-expansion concept any longer. Series-expansion methods are iterative algorithms characterized by slow convergence and thus they reconstruct images much slower than the transform methods. However, the development of very fast and efficient computers may make it possible to shorten the computation time, which will give an advantage to series-expansion methods [1] because of:

— their wide application range regardless of the measurement geometry and the kind of data,

— the possibility of reconstructing high-contrast images of the structure of objects characterized by sudden changes in density, which is essential for the application of tomography to industrial non-destructive testing,

— the possibility of reconstructing an image in the case of a small number of illumination angles or incomplete projections.

But at the moment, the long computation time required by series-expansion methods makes it impossible to increase the number of iterations significantly (it is still not possible to implement series-expansion methods on PCs) and so the images reconstructed by these methods are often obscured by noise and distorted [2, 5]. The much bigger errors occurring here than in the case of transform methods are due to the assumption of a linear energy propagation path between the source and the detector, which for UTT is a serious shortcoming because of refraction. Thus one can say that at the moment, the transform algorithm is the most suitable for UTT.

Among transform algorithms one can distinguish two basic types: operating in the space domain (the convolution and backprojection algorithm [6]) and operating in the domain of spatial frequencies (the Fourier inversion and the filtered backprojection algorithm [6]). Considering that the two types have a common origin, it is surprising that they differ radically in their operation. The convolution and backprojection algorithm is highly versatile. Being currently one of the most effective algorithms, it is used in the latest models of computer X-ray tomographs. It has been superseding the Fourier versions. The reason for its dominance is mainly the ease with which it can be implemented in both the software and hardware applications and the fact that it makes it possible to obtain sharp high-quality images from noise-free measuring data [6]. Algorithms based on the Fourier transform are not so easy to implement because of two-dimensional interpolation which lowers the quality of the image [6, 7]. Whereas calculation of the Fourier transforms have this advantage that they require a potentially smaller number of computations to reconstruct an image. Unfortunately, calculation of Fourier transforms, whose efficiency makes this method attractive, are also a source of its shortcomings [2]. Fourier algorithms require direct estimates of the complex amplitude of image harmonic components and an error in one of the components degrades the whole image [6]. The cause of such errors may be inaccurate interpolation. In the convolution and backprojection algorithm inaccurate interpolation is harmless — it causes only smoothing of the image [6].

To take a final decision about the choice of an algorithm, the reconstruction of a simple object by means of the Fourier inversion algorithm and the convolution and backprojection algorithm was considered. Let the object be described by a function which

assumes the value of 1 within a circle with radius a and 0 outside this circle. The Fourier transform of such an object is an oscillating function with the oscillation becoming faster as the object's size increases or when the object is for away from the origin of the image co-ordinates. Faster oscillations of the function result in a bigger error introduced by simple interpolation between the function samples. In the convolution and backprojection method interpolation takes place for convolved data. For the sampled projections of the considered object it can be stated that the sampled convolved data are close to theoretical results. This means that, regardless of the size of an object or its position relative to the origin of the image co-ordinates, a negligible interpolation error appears in the reconstructed values within the circle.

To sum up, the convolution and backprojection algorithm, adapted and tested in this research, is the most suitable one for UTT purposes.

3. Convolution and backprojection algorithm

The convolution and backprojection algorithm was brought out by Ramachandran and Lakshminarayanan in 1971 [11] and later popularized by Shepp and Logan [12]. The reconstruction method here is similar to the filtered backprojection algorithm [5, 6], except that filtration takes place in the space domain (as a convolution) and not in the domain of spatial frequencies, which naturally eliminates the problems connected with FFT. The initial convolution and backprojection algorithm formula has this form [6]:

$$f_B(x,y) = \int_0^{\pi} \int_{-1}^{1} p(s,\psi) q(x\cos\psi + y\sin\psi - s)\, ds\, d\psi, \tag{1}$$

where

$$q(s) = \int_{-1/2\Delta s}^{1/2\Delta s} |R| W(R) e^{j2\pi Rs}\, dR, \tag{2}$$

and $p(s,\psi) = p_\psi(s)$ are the measuring data collected in a parallel ray projection geometry (Fig. 1), $W(R)$ is a window function, f_B — band-limited approximation of function $f(x,y)$, and s is normalized to area $[-1,1]$. Formula (1) can be separated into two parts:

$$\widetilde{p}(s',\psi) = \int_{-1}^{1} p(s,\psi) q(s'-s)\, ds, \tag{3}$$

$$f_B(x,y) = \int_0^{\pi} \widetilde{p}(x\cos\psi + y\sin\psi, \psi)\, d\psi. \tag{4}$$

Formula (3) is an outcome of the convolution of projections at an angle of ψ and convolving function $q(s)$ defined by general formula (2) (different convolving functions are obtained for different window functions). Formula (4) is known as backprojection and it has a simple geometric interpretation. The arguments of the function described by

equation (3) are parameters of a ray passing through point (x, y) at angle ψ, which means that function $f(x, y)$ is created by integrating values of the convolved projection accompanying all the rays passing through point (x, y).

In practical reconstruction-from-projection applications, the measuring data correspond to estimates $p(s, \psi)$ for many discrete values s and ψ and the reconstructed image is generated in the form of a two-dimensional table of numbers. The principles which apply to the optimization of a reconstruction algorithm on the basis of discrete data should be considered for a case when p is sampled cocurrently for s and ψ. If we have a set of projections measured at N angles spaced at $\Delta\psi$ by means of M rays spaced at Δs, then for each of N projections we can determine constant integers M^+ and M^-:

$$\left.\begin{array}{rcl} M^+ &=& (M-1)/2 \\ M^- &=& -(M-1)/2 \end{array}\right\} \quad \text{for odd } M, \tag{5}$$

$$\left.\begin{array}{rcl} M^+ &=& (M/2)-1 \\ M^- &=& -M/2 \end{array}\right\} \quad \text{for even } M. \tag{6}$$

To make sure that set of rays $\{(m\Delta s, n\Delta\psi) : M^- \le m \le M^+,\ 1 \le n \le N\}$ covers a unit circle (a normalized measuring area), one should choose $\Delta\psi = \pi/N$ and $\Delta s = 1/M^+$ from the whole range of directions. In this way one can refer to set $p(m\Delta s, n\Delta\psi)$ as to parallel-ray data. A Cartesian grid of image point values is defined as set $\{(k\Delta x, l\Delta y) : K^- \le k \le K^+,\ L^- \le l \le L^+\}$ where numbers K^-, K^+, L^-, L^+ are defined in the same way as M^- and M^+ (formulas (5), (6)). A reconstruction algorithm should generate estimates $f(k\Delta x, l\Delta y)$ for $K \times L$ image points from $M \times N$ measurements $p(m\Delta s, \psi_n)$ for $\psi_n = n\Delta\psi$. Thus an algorithm performing approximation $f_B(k\Delta x, l\Delta y)$ on the basis of projection data $p(m\Delta s, \psi_n)$ is needed. The simplest way in which backprojection integrals (formula (4)) can be determined is to apply the trapezoid rule [6]:

$$f_B(k\Delta x, l\Delta y) \cong \Delta\psi \sum_{n=1}^{N} \widetilde{p}(k\Delta x \cos\psi_n + l\Delta y \sin\psi_n, \psi_n). \tag{7}$$

Then for each angle ψ_n one should find convolved projection values $\widetilde{p}(s', \psi_n)$ for set $K \times L$ of values s'. A practical approach to this problem is to estimate $\widetilde{p}(s', \psi_n)$ for $M^- \le m \le M^+$ projections and then to apply reasonable interpolation to calculate $K \times L$ values $\widetilde{p}$ on the basis of only M calculated convolved values. Thus the convolution (formula (3)) should be expressed in two stages: a discrete convolution whose result is written as $\widetilde{p}_C$, followed by interpolation $\widetilde{p}_I$. These operations are represented by a pair of equations [6]:

$$\widetilde{p}_C(m'\Delta s, \psi_n) = \Delta s \sum_{m=M^-}^{M^+} p(m\Delta s, \psi_n) q((m'-m)\Delta s) \quad \text{for } M^- \le m' \le M^+, \tag{8}$$

$$\widetilde{p}_I(s', \psi_n) = \Delta s \sum_{m'} \widetilde{p}_C(m'\Delta s, \psi_n) I(s' - m'\Delta s), \tag{9}$$

where $s' = k\Delta x \cdot \cos\psi_n + l\Delta y \cdot \sin\psi_n$ and $I(s)$ is an interpolation function. If linear interpolation of convolved values is assumed, function $I(s)$ can be written as:

$$I_L(s) = \begin{cases} \dfrac{1}{\Delta s}(1 - |s|/\Delta s), & |s| \le \Delta s, \\ 0, & |s| \ge \Delta s. \end{cases} \tag{10}$$

There are many convolving functions which can be used in a convolution and backprojection algorithm. One of the most often used is the following function [6]:

$$q(m\Delta s) = \begin{cases} \dfrac{3 - 2E}{12(\Delta s)^2} & \text{for } m = 0, \\ -\dfrac{E}{\pi^2(m\Delta s)^2} & \text{for even } m, \\ -\dfrac{1 - E}{\pi^2(m\Delta s)^2} & \text{for odd } m, \end{cases} \tag{11}$$

where $0 \le E \le 1$ is a convolving function parameter. A special case of this convolving function is the Ram-Lak (Ramachandran and Lakshminarayanan) function [4]:

$$q_{RL}(m\Delta s) = \begin{cases} \dfrac{1}{4\Delta s^2} & \text{for } m = 0, \\ \dfrac{-\sin^2(\pi m/2)}{\pi^2 m^2 \Delta s^2} & \text{for } m \ne 0, \end{cases} \tag{12}$$

obtained from formula (11) for parameter $E = 0$. Another frequently used function is the Shepp-Logan function [4]:

$$q_{SL}(m\Delta s) = \frac{2}{\pi^2 \Delta s^2 (1 - 4m^2)}\,. \tag{13}$$

The convolution and backprojection algorithm is simple to implement, quite accurate and fast. It is currently used in the latest models of computer X-ray tomographs as one of the most effective algorithms.

4. Measuring data fitting

For the convolution and backprojection algorithm four basic assumptions, which must be satisfied to obtain a correctly reconstructed image, hold good:

1) parameter values measured in projections (entered into the algorithm) constitute an integral of local values over the ultrasonic beam's path,

2) the path between the source and the detector is a straight line,

3) values measured outside the measuring area are zero,

4) measuring data entered into the algorithm operating on a measuring circle having a radius of 1, placed in the centre of the co-ordinate system must be re-scaled appropriately.

For the measurement of the time t_p in which an ultrasonic wave passes through the object, the local values are the inverses of sound velocity $1/c(x, y)$ (condition **1**)):

$$t_p = \int\limits_L dt_p = \int\limits_L \frac{dt_p}{dl}\, dl = \int\limits_L \frac{1}{c(x, y)}\, dl. \tag{14}$$

Condition **2**) can be satisfied only approximately by assuming that for the measured objects, the elongation (as a result of refractions) of the ultrasonic wave propagation path from the transmitter to the receiver is negligible. Measurement of the circle diameter d_p in a parallel ray projection geometry is determined either by the tracking range or by sending transducer-receiving transducer distance l_o:

$$d_p = \begin{cases} (M-1)\Delta s & \text{for } (M-1)\Delta s < l_o\,, \\ l_o & \text{for } (M-1)\Delta s \geq l_o\,, \end{cases} \tag{15}$$

where M stands for a number of measuring rays spaced at Δs. According to condition **3**), measurement values outside a circle of diameter d_p should be zero. This condition can be fulfilled in the simplest way by entering reduced time T_d, i.e. difference $t_p - t_{\text{med}}$, instead of the measured transition time values t_p, into the algorithm, where time t_{med} is the time in which an ultrasonic wave passes through a measuring medium (water) at distance l_o (assuming that $t_{\text{med}} \cong \text{const}$). To satisfy condition **4**), let us consider scaling two different parameters entered into the convolution and backprojection algorithm, specified as method A: T_d and method B: $-c_{\text{med}} \cdot T_d$, when for the two parameters assumptions **1**)–**3**) hold good. If the reduced time measured over path l_o is T_d, the reduced time over path **2** is:

$$\widehat{T}_d = \hat{t}_p - \hat{t}_{\text{med}} = \frac{2t_p}{l_o} - \frac{2t_{\text{med}}}{l_o} = \frac{2}{c_p} - \frac{2}{c_{\text{med}}}\,, \tag{16}$$

where c_p stands for mean ultrasonic wave propagation values measured in a parallel ray projection geometry at distance l_o, and c_{med} is a mean ultrasonic wave propagation velocity in a measuring medium, measured at distance l_o. It is easy to prove that

$$\begin{aligned} \widehat{T}_d = \frac{2}{c_p} - \frac{2}{c_{\text{med}}} = \int_{-1}^{1} \left(d\hat{t}_p - d\hat{t}_{\text{med}}\right) = \int_{-1}^{1} \left(\frac{d\hat{t}_p}{dl} - \frac{d\hat{t}_{\text{med}}}{dl}\right) dl \\ = \int_{-1}^{1} \left(\frac{1}{c(x,y)} - \frac{1}{c_{\text{med}}}\right) dl = \int_{-1}^{1} f^{(A)}(x,y)\, dl. \end{aligned} \tag{17}$$

In the case of method A, to reproduce, after reconstruction, the local ultrasonic wave propagation velocities, values $2/c_p - 2/c_{\text{med}}$ should be entered into the convolution and backprojection algorithm and the following recalculation should be done for each reconstructed value $f^{(A)}(x,y)$:

$$c(x,y) = \frac{1}{f^{(A)}(x,y) + \dfrac{1}{c_{\text{med}}}}\,. \tag{18}$$

In method B the difference lies in the fact that after re-scaling as above, we enter values $2 \cdot (1 - c_{\text{med}}/c_p) = 2 \cdot (1 - n_p)$ (where n_p is a mean value of the refraction index [5]) into the algorithm and after reconstruction and recalculation we get:

$$c(x,y) = \frac{c_{\text{med}}}{-f^{(B)}(x,y) + 1}\,. \tag{19}$$

The two above methods were verified by reconstructing an image on the basis of simulated tomographic measurements of the mean velocity of the propagation of an ultrasonic wave in a cross-section of a homogenous cylinder immersed in water (Fig. 2): identical results were obtained.

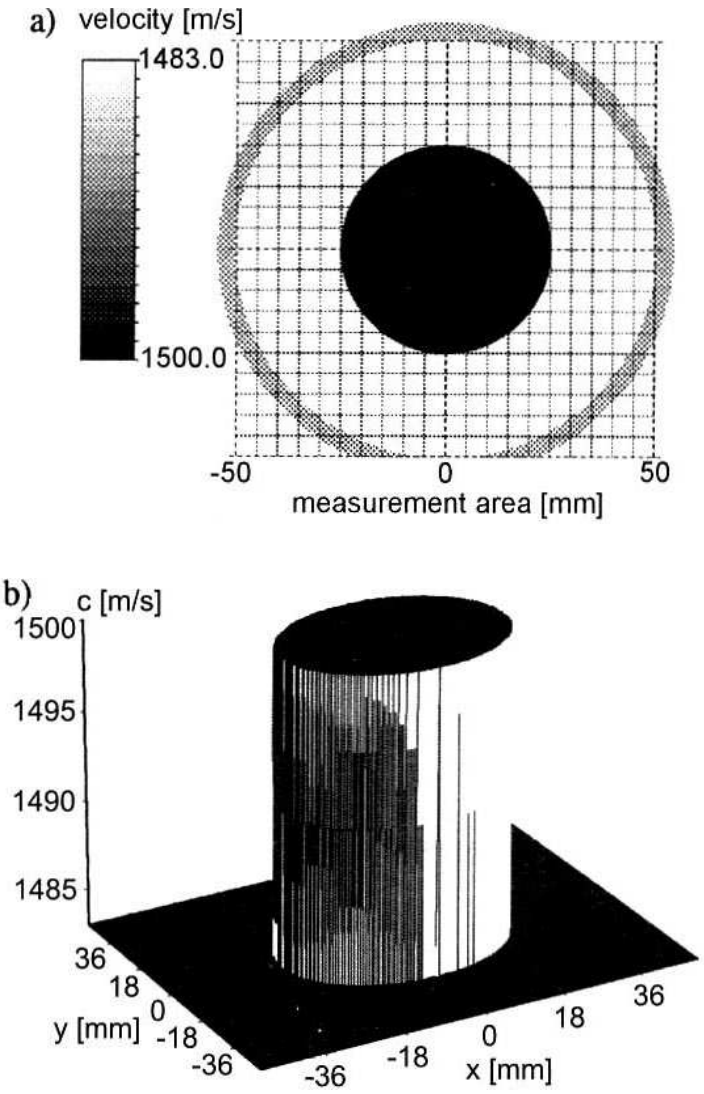

Fig. 2. Image of assigned cylinder cross-section in: a) gray scale, b) pseudo-3D. The following parameters were assigned: sound velocity in cylinder — 1500 m/s, sound velocity in water — 1483 m/s, cylinder's diameter — 50 mm, measuring circle's diameter — $d_p = l_o = 100$ mm.

In the further research method B was used for reconstruction calculations because of shorter computation time.

5. Optimization

The convolution and backprojection algorithm was subjected to optimization through the selection of a convolving function. Two functions: $q(m\Delta s)$ [6] for several values of parameter E and Shepp-Logan function $q_{SL}(m\Delta s)$ (formulas (11), (13)) were tested. The considered convolving functions are shown in Fig. 3 for discrete values $m \cdot \Delta s$. In the case of function $q(m\Delta s)$, calculation were done for seven values of parameter $E = 0$, 0.2, 0.4, 0.5, 0.6, 0.8, 1.

Images of an assigned cylinder cross-section (Fig. 2) were reconstructed by means of the convolution and backprojection algorithm using each of the convolving functions shown in Fig. 3. The obtained images in pseudo-3D are shown in Fig. 4.

If one compares the shapes of the convolving functions (Fig. 3), one can notice that the Shepp-Logan function is very similar to function q with parameter $E = 0.2$, 0.4. The similarity is also visible in the case of the reconstructed images of the cylinder cross-section (Fig. 4). This means that convolving function $q(m \cdot \Delta s)$, presented in a paper by R.M. Lewitt [6] (formula (11)), is a highly versatile function. Thus there is no need to use many different convolving functions in the convolution and backprojection algorithm since the effects which they produce can be brought about by changing the value of parameter $0 \leq E \leq 1$ of function q. Being able to change the value of parameter E, one can reconstruct images differing in contrast.

For low values of parameter $E \leq 0.4$ one can obtain very sharp images with clearly visible edges at structural boundaries (Fig. 4 a – c), in which local sound velocities are meticulously reconstructed in comparison with the object (Fig. 4a). A drawback of this kind of reconstruction are oscillations of the reconstructed values close to the measuring-area boundary (Fig. 4a – c) and interference in the imaging of any discontinuities manifesting itself in overstated reconstructed values at boundaries (Fig. 4 a – c).

For high values of parameter $E \geq 0.6$ images are less contrasty, which manifests itself in blurring of the boundaries of any discontinuities in the reconstructed structure (Fig. 4 e – g). Thus the reconstructed values close to such boundaries contain significant errors. This kind of reconstruction has, however, an advantage: no oscillation in image values close to the measuring area boundary and no interference in the imaging of discontinuities (Fig. 4 e – g). For parameter $E = 0.5$ the above effects for low and high values are balanced (Fig. 4d).

Reconstruction errors along image line $y = 0$ for parameter $E = 0$ and $E = 1$ at $M = 101$ rays and $N = 160$ projections are given in Fig. 5. As regards the image sharpness, it is more advantageous to use low values of E but if the aim is to minimize the offset of reconstructed image point values relative to the assigned values, it is better to use high values of E.

A nonlinear interpolation function can be used to improve the quality of imaging since if linear interpolation is adopted (formula (10)) in the convolution and backprojection algorithm, two kinds of interference occur [6]:

— the reconstructed function is a locally smooth version of the original object function,

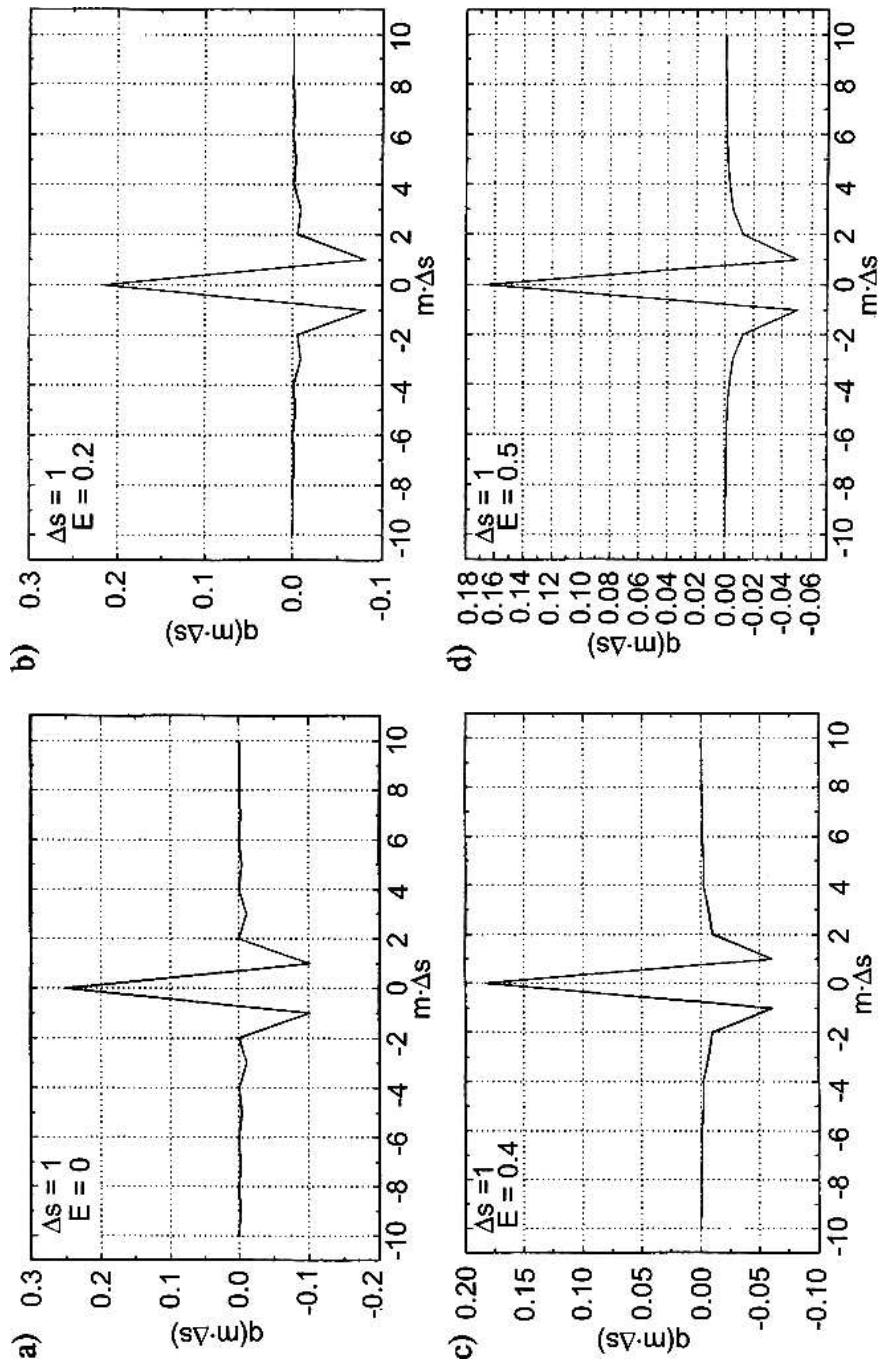

[Fig. 3]

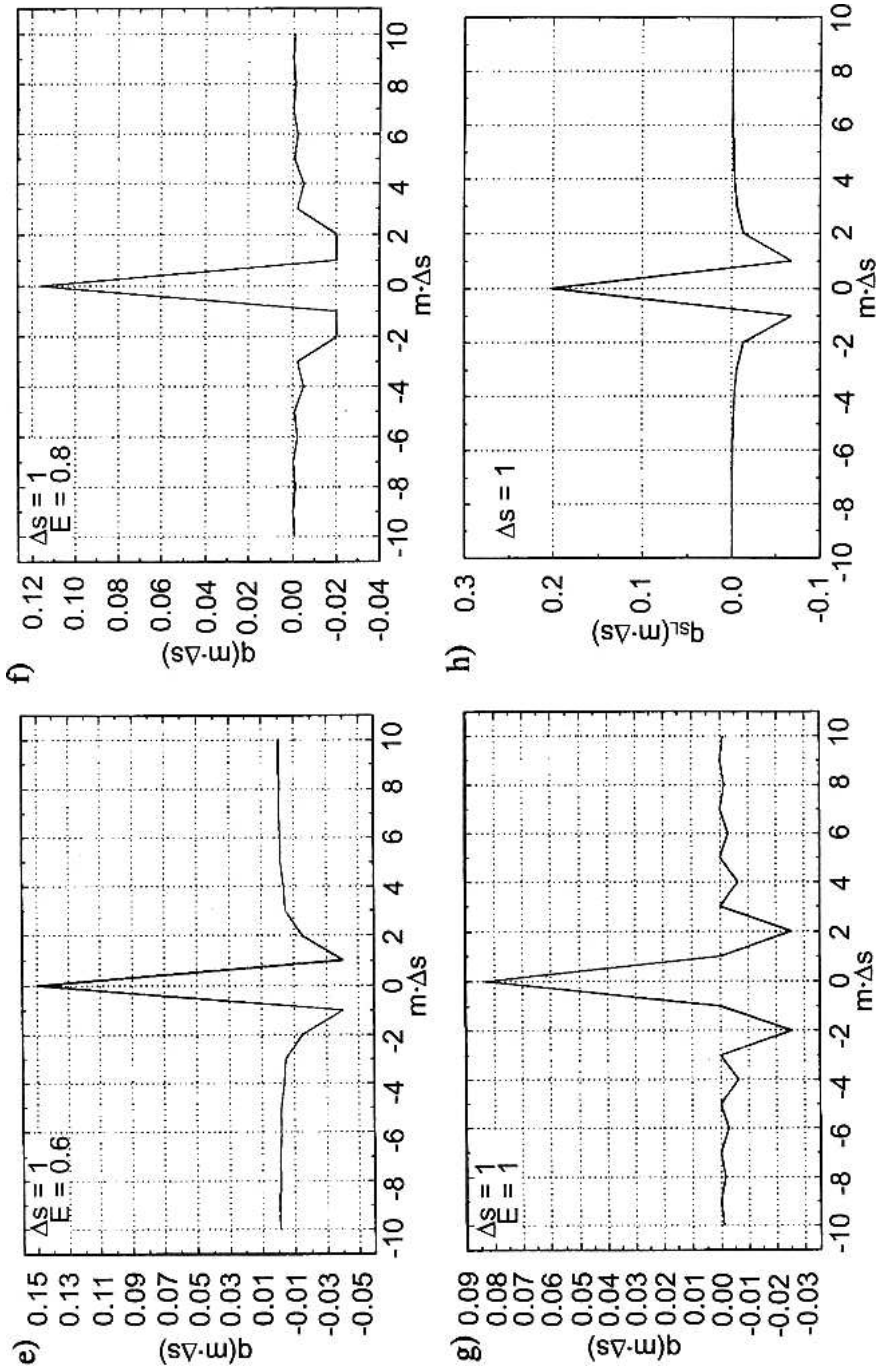

Fig. 3. Convolving functions for discrete data, function q acc. to formula (11) for parameter: a) $E = 0$ (Ram-Lak function, formula (12)), b) $E = 0.2$, c) $E = 0.4$, d) $E = 0.5$, e) $E = 0.6$, f) $E = 0.8$, g) $E = 1$, h) Shepp-Logan function (formula (13)).

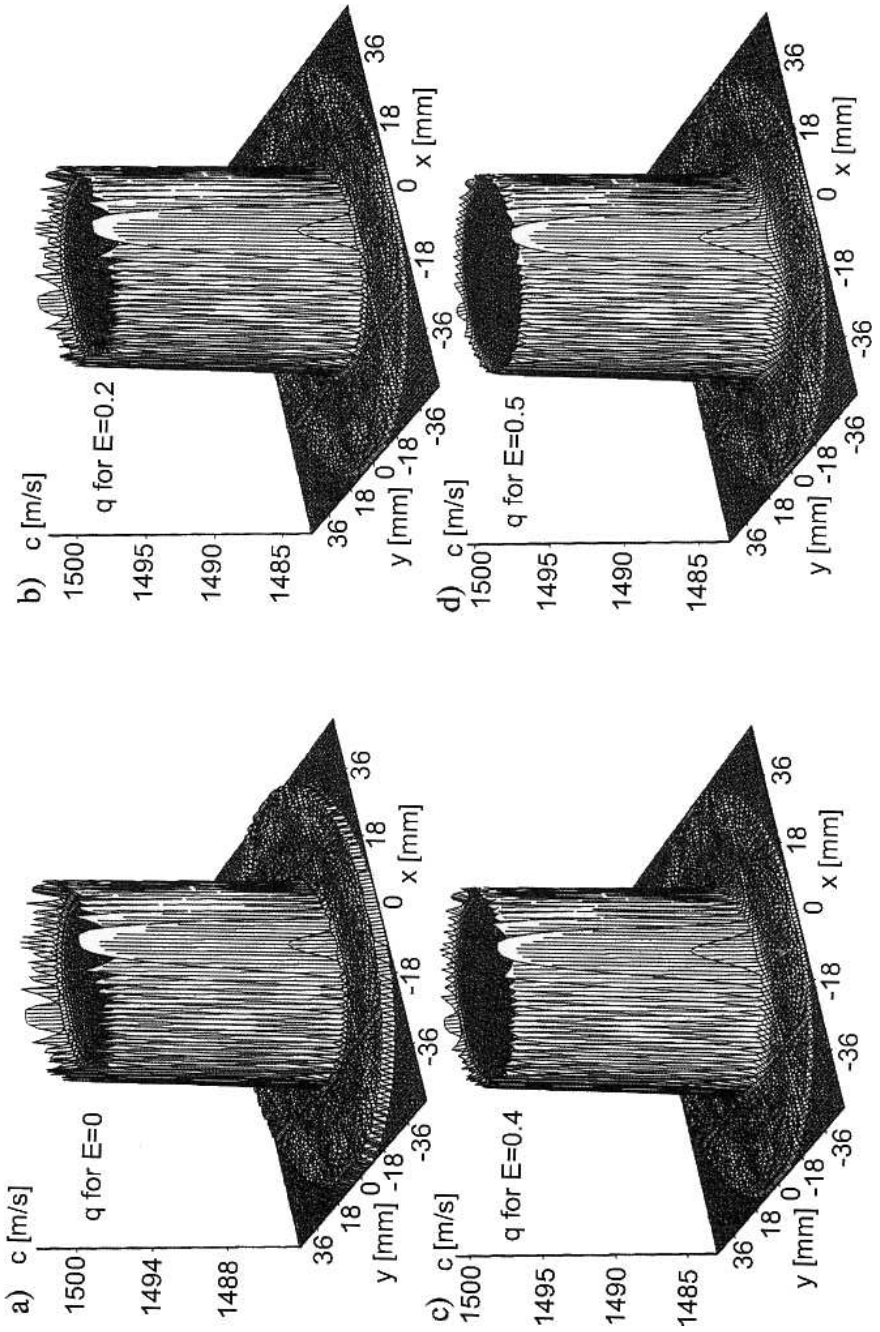
a) c [m/s]
q for E=0
1500
1494
1488
b) c [m/s]
q for E=0.2
1500
1495
1490
1485
c) c [m/s]
q for E=0.4
1500
1495
1490
1485
d) c [m/s]
q for E=0.5
1500
1495
1490
1485
y [mm]
x [mm]
36
18
0
-18
-36

[Fig. 4]

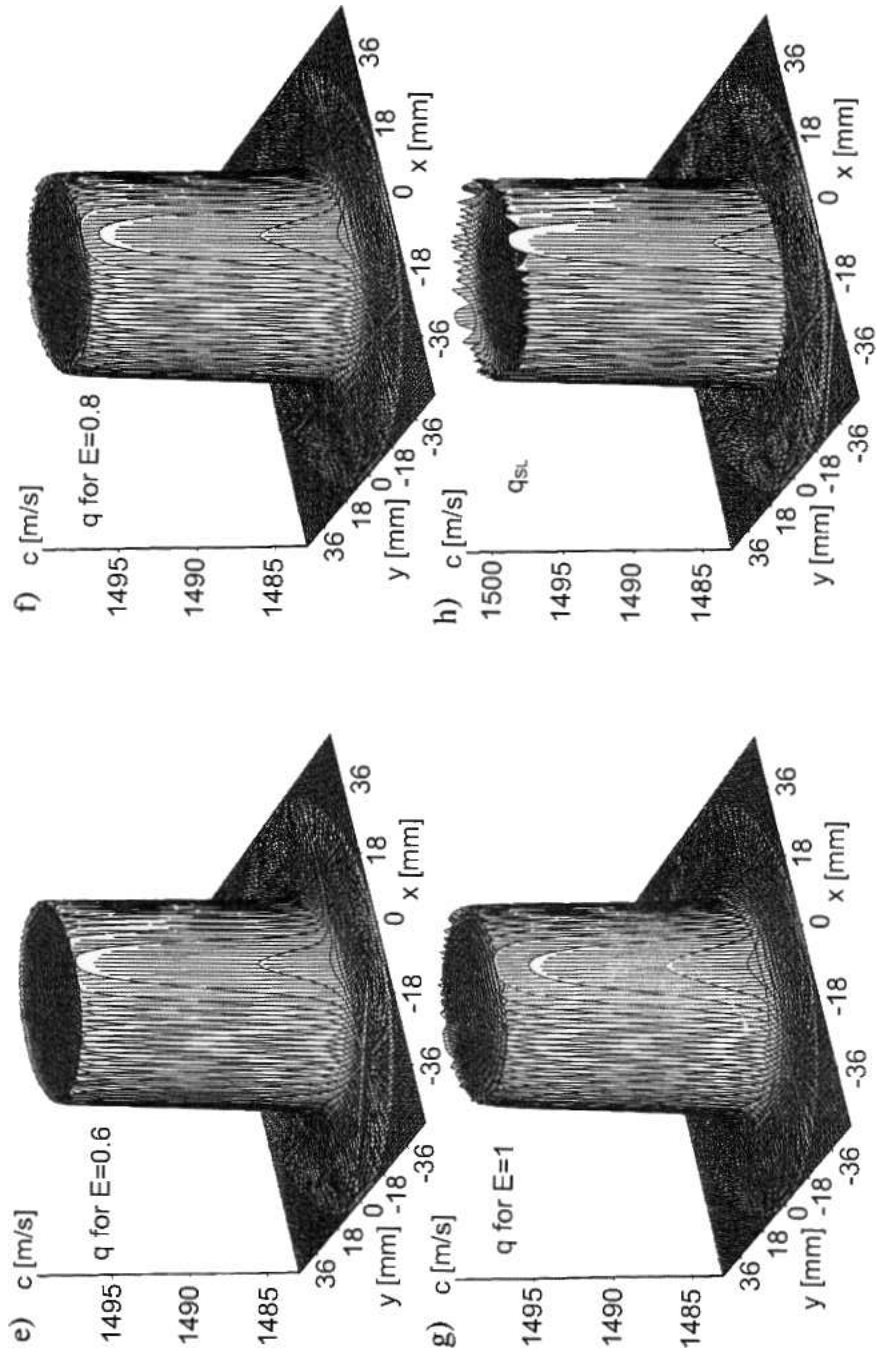

Fig. 4. Cylinder cross-section (from Fig. 2) images reconstructed by means of convolution and backprojection algorithm for different convolving functions, presented in pseudo-3D: a) $q_{E=0}$, b) $q_{E=0.2}$, c) $q_{E=0.4}$, d) $q_{E=0.5}$, e) $q_{E=0.6}$, f) $q_{E=0.8}$, g) $q_{E=1}$, h) q_{SL}.

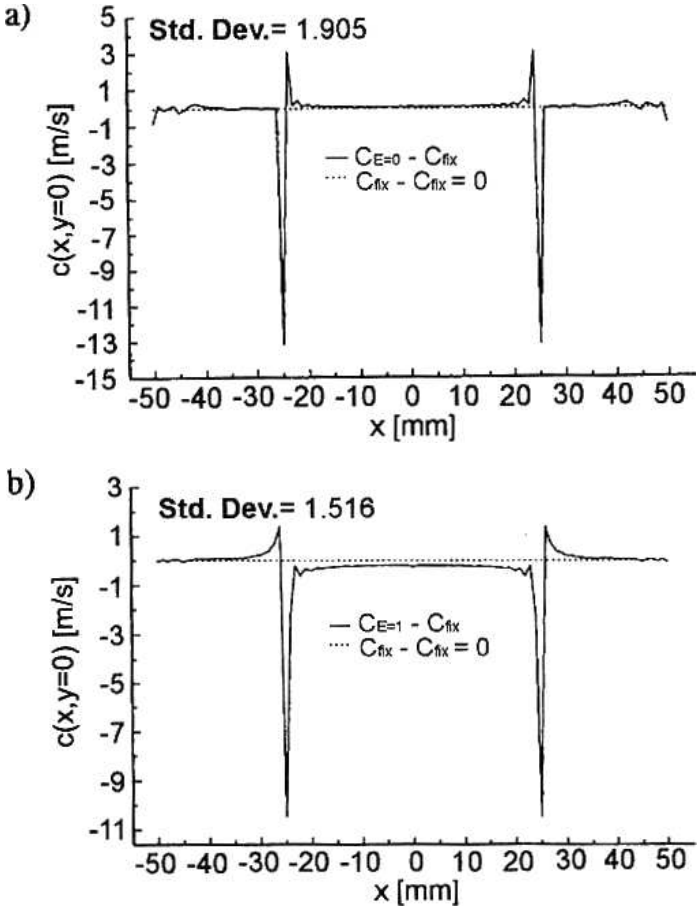

Fig. 5. Reconstruction errors along image line $y = 0$: a) for parameter $E = 0$, b) for parameter $E = 1$, at $M = 101$ rays and $N = 160$ projections (standard deviations have been marked).

— the reconstructed function is characterized by rapid variation of values and their derivatives.

Nevertheless, the smoothing effect is relatively harmless since it is equivalent, in principle, to the modification of convolving function q by increasing the value of parameter E. Thus it can be eliminated by lowering the value of E. The oscillation effect in the reconstructed image manifests itself as streaks radiating from sharp edges (Fig. 4 a–f, h). This interference is not serious enough to justify the introduction of a complicated nonlinear interpolation function since this would extend the reconstruction computation time considerably.

In the further research only the convolution and backprojection algorithm in conjunction with convolving function $q(m \cdot \Delta s)$ (formula (11)) and linear interpolation function $I_L(s)$ (formula (10)) is used. Such a value of the convolving function parameter was chosen which ensured images of the best possible quality (in most cases: $E = 0$ and $E = 1$).

6. Testing

To determine a minimum number of measuring data (rays and projections) and to choose an optimum reconstruction grid size — the parameters which determine the quality of an image — the convolution and backprojection algorithm was tested by simulated tomographic measurements of a cylinder cross-section (Fig. 2). For the convolution and backprojection algorithm it is possible to derive a formula for the interrelationship between the number of rays M and the number of projections N, which is necessary in order to minimize the reconstructed image distortions introduced by the algorithm [6]:

$$N - 1 > \frac{\pi M}{2} \,. \tag{20}$$

This criterion provides many useful guidelines for many applications, considering that the effects of sampling in domain s and in domain ψ interact in a complicated way.

Figure 6 shows image distortions due to an insufficient number of projections relative to the number of rays (Fig. 6 a – c). It is enough to satisfy condition (20) to obtain good-quality images (Fig. 6f). By further increasing the number of projections only slight smoothing of image point value oscillations is obtained (Figs. 6 g, h). It is surprising that a quite clear image can be obtained already for the number of projections smaller by half than the number of rays (Fig. 6d). It should be noted, however, that the tested object is homogenous and large. In the case of objects with complex internal structure, it may become necessary to use the maximum number of projections determined by condition (20) in order to obtain a good-quality image [8 – 10].

Figures 7 and 8 show how the reconstructed image of the object's cross-section changes depending on the number of measuring rays if condition (20) is fulfilled. In the case of the tested object, a highly accurate image can be obtained already for 101 rays (Figs. 7 e, 8 e) and an undisturbed shape of the object's cross-section — for about 30 rays (Figs. 7 c, d and 8 c, d). By further increasing the number of rays only the interference at structural boundaries is minimized (Figs. 7 f – h and 8 f – h). Thus the cross-section of each homogenous structure can be visualized with high accuracy by means of the convolution and backprojection algorithm, assuming $M \geq 51$ rays for its largest dimension and $N \geq 81$ projections, if we have error-free measurements of the mean values of the acoustic parameter being determined, obtained in a parallel ray projection geometry.

The convolution and backprojection algorithm reconstructs an image as set $K \times L$ of values. This set is called a Cartesian image reconstruction grid. Grid size can be chosen depending on needs. Normally, an equal number of points K in the horizontal plane and points L in the vertical plane is assumed to obtain an area of the image without any differentiation of its resolution along axis X or Y. If the reconstructed image is presented in the gray scale, its resolution is determined by the monitor's or the printer's resolution. Grid size also depends on number M of measuring rays. If grid size $K = L$ is larger than number M of the rays, then the reconstructed image becomes blurred (Fig. 9 b–d) due to the considerable influence of the interpolation of the convolved values. For grid size equal to the number of measuring rays, each pixel of the reconstructed image is a square with

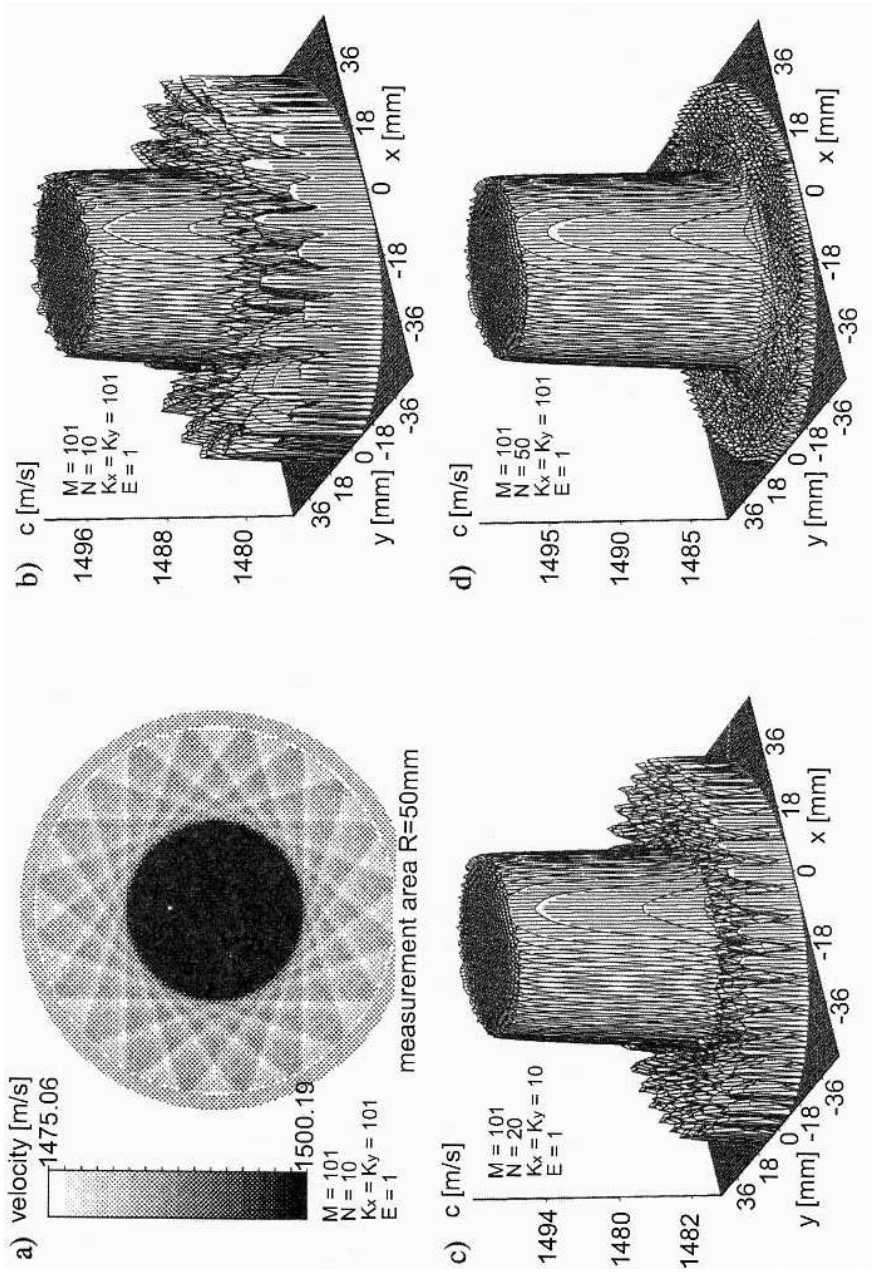
a) velocity [m/s]
1475.06
1500.19
M = 101
N = 10
Kx = Ky = 101
E = 1
measurement area R=50mm
b) c [m/s]
M = 101
N = 10
Kx = Ky = 101
E = 1
1496
1488
1480
y [mm]
x [mm]
c) c [m/s]
M = 101
N = 20
Kx = Ky = 10
E = 1
1494
1480
1482
d) c [m/s]
M = 101
N = 50
Kx = Ky = 101
E = 1
1495
1490
1485

[Fig. 6]

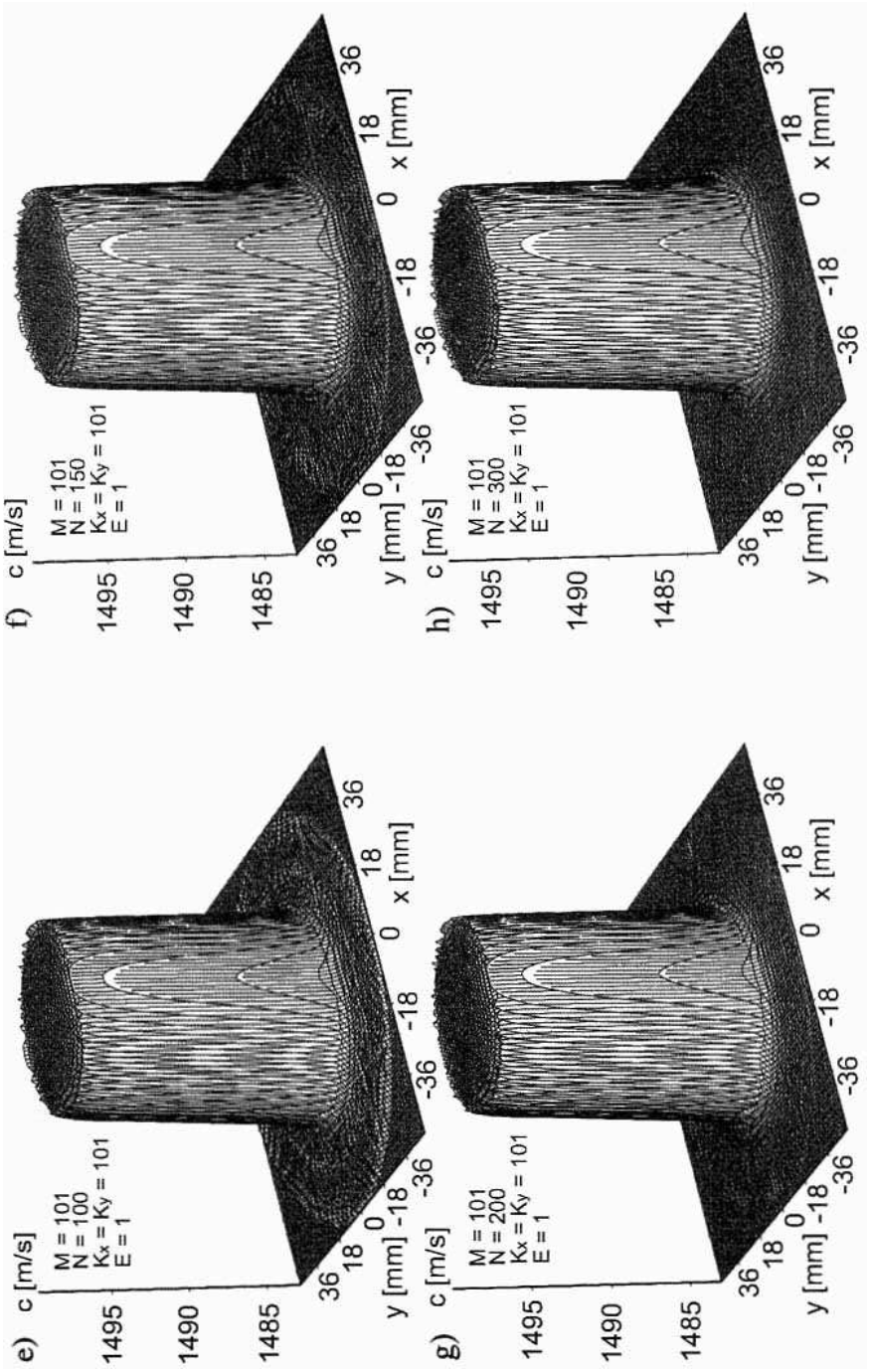

Fig. 6. Cylinder cross-section (from Fig. 2) images reconstructed by means of convolution and backprojection algorithm for $M = 101$ rays and different number of measuring projections N, shown in gray scale a) and in pseudo-3D b)–h) for $E = 1$.

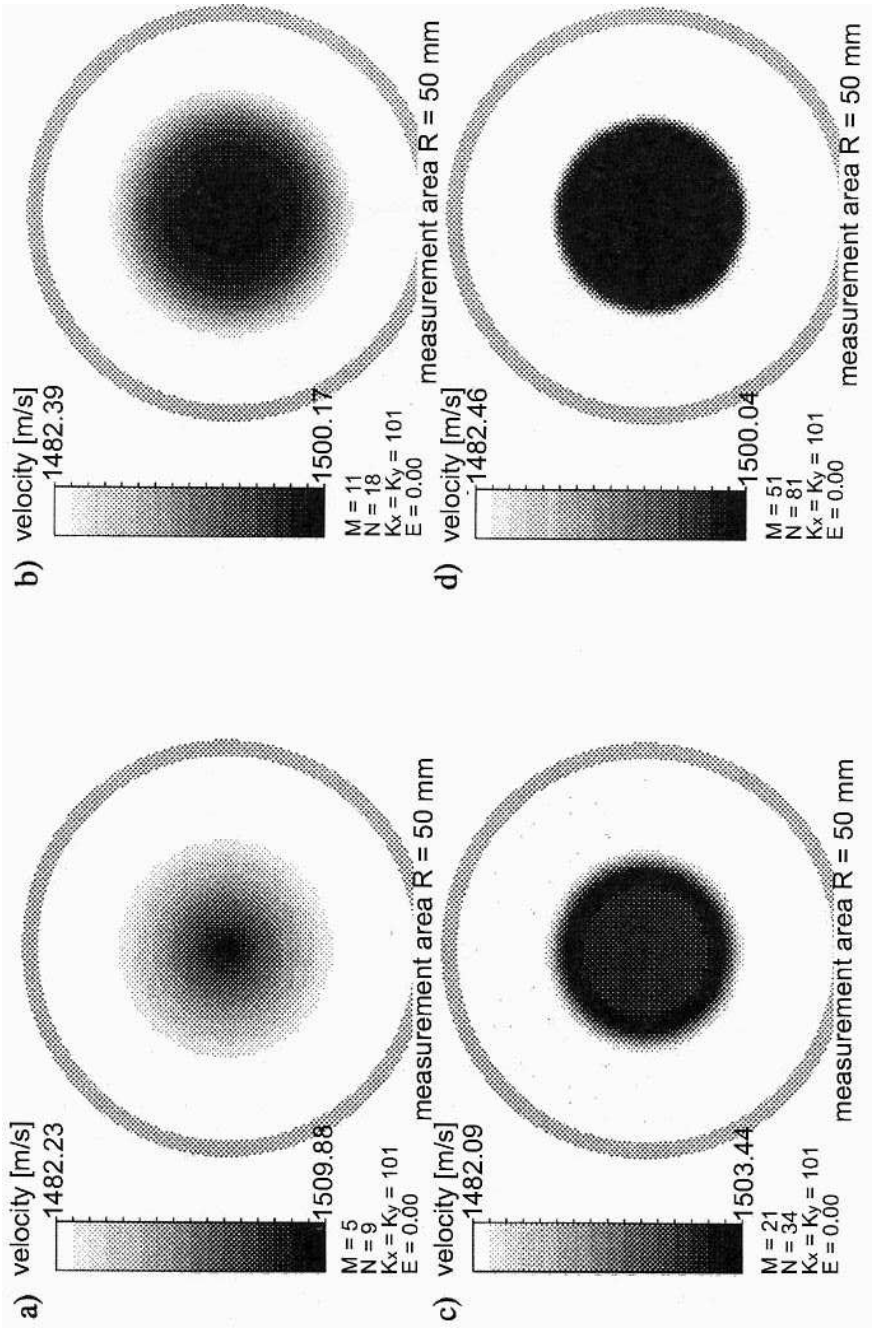
a)
velocity [m/s]
1482.23
1509.88
M = 5
N = 9
Kx = Ky = 101
E = 0.00
measurement area R = 50 mm
b)
velocity [m/s]
1482.39
1500.17
M = 11
N = 18
Kx = Ky = 101
E = 0.00
measurement area R = 50 mm
c)
velocity [m/s]
1482.09
1503.44
M = 21
N = 34
Kx = Ky = 101
E = 0.00
measurement area R = 50 mm
d)
velocity [m/s]
1482.46
1500.04
M = 51
N = 81
Kx = Ky = 101
E = 0.00
measurement area R = 50 mm

[Fig. 7]

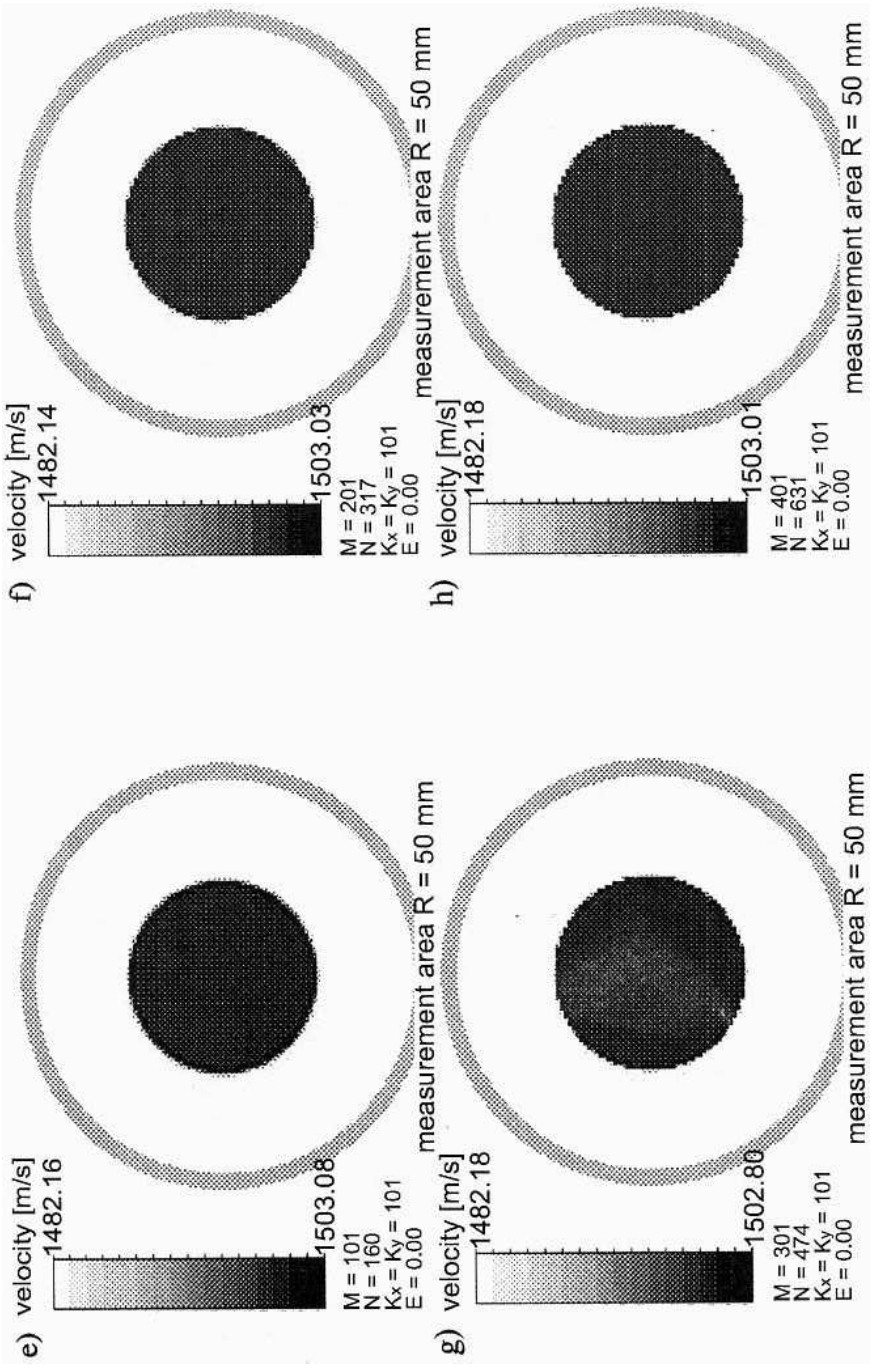

Fig. 7. Cylinder cross-section (from Fig. 2) images reconstructed by means of convolution and backprojection algorithm for different number of measuring rays and minimum required number of projections (acc. to formula (20)), shown in gray-scale for $E = 0$.

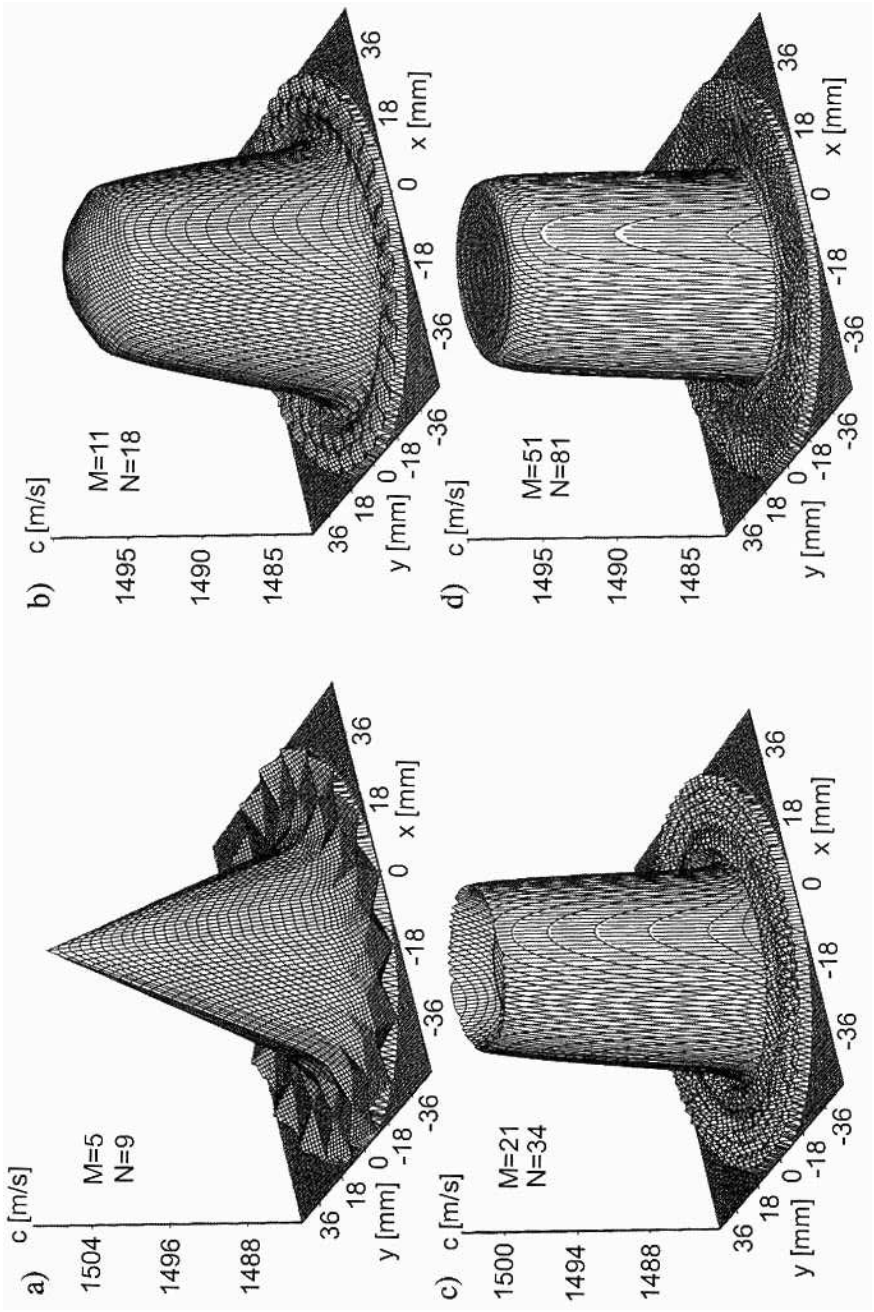
a)
c [m/s]
M=5
N=9
1504
1496
1488
b)
c [m/s]
M=11
N=18
1495
1490
1485
c)
c [m/s]
M=21
N=34
1500
1494
1488
d)
c [m/s]
M=51
N=81
1495
1490
1485
y [mm]
x [mm]
36
18
0
-18
-36

[Fig. 8]

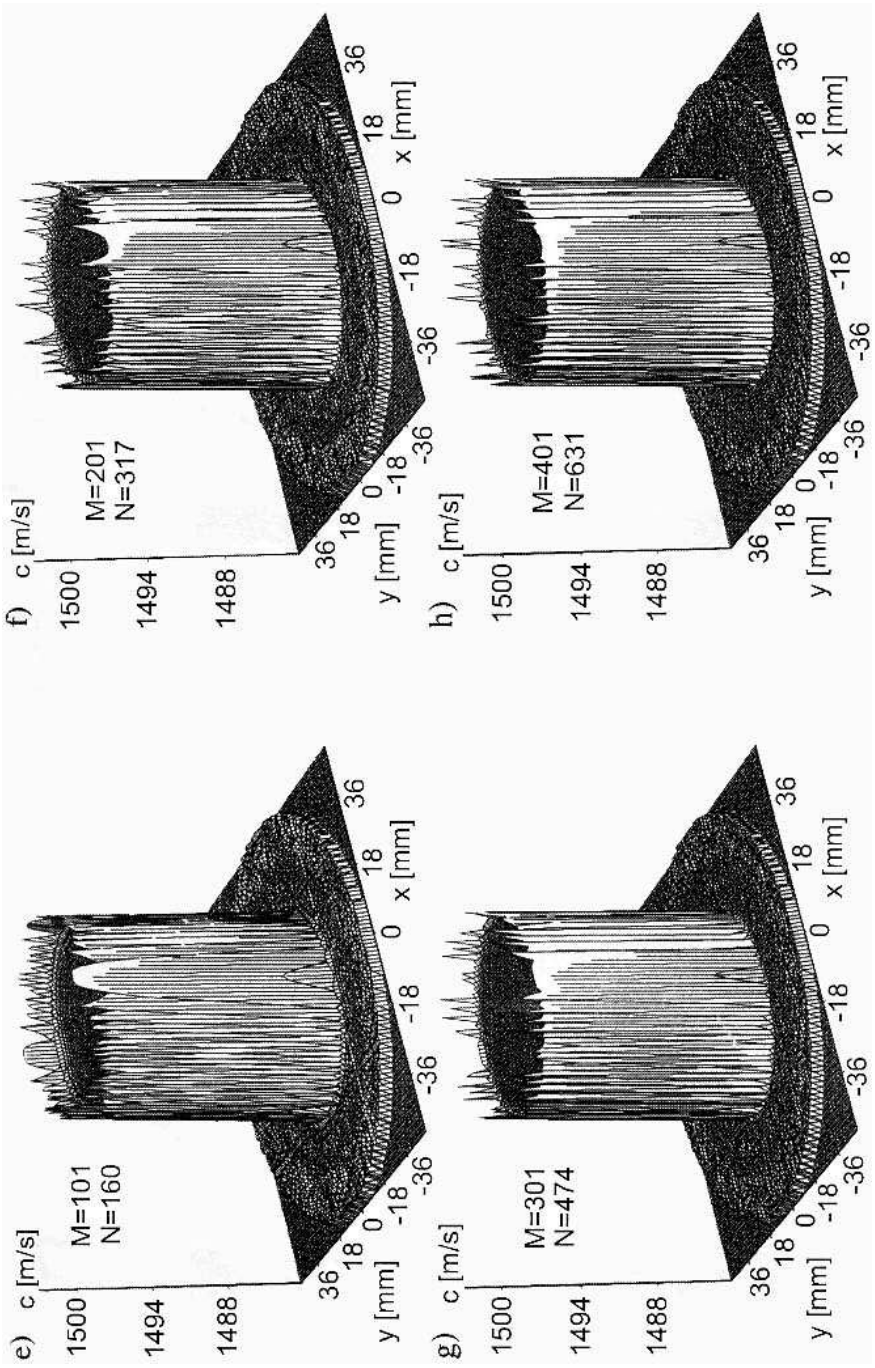

Fig. 8. Cylinder cross-section (from Fig. 2) images reconstructed by means of convolution and backprojection algorithm for different number of measuring rays and minimum required number of projections (acc. to formula (20)), shown in pseudo-3D for $E = 0$.

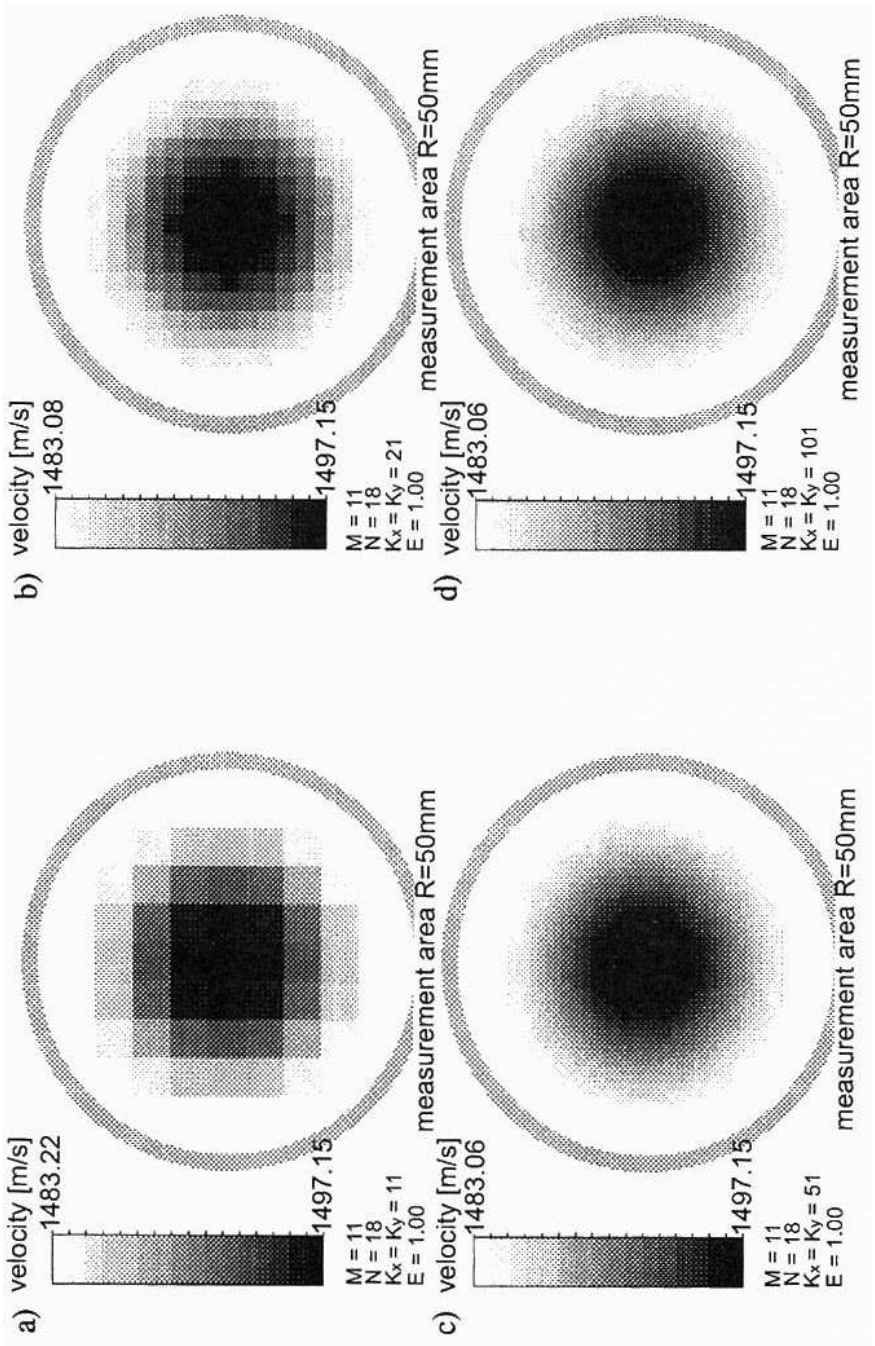

Fig. 9. Cylinder cross-section (from Fig. 2) images reconstructed by means of convolution and backprojection algorithm, shown in gray scale for different image reconstruction grid sizes ($E = 0$).

side Δs (Fig. 9 a) where Δs stands for a transducer tracking jump. The larger the grid size (small size of pixels), the longer the reconstruction computation time. Therefore a reasonable grid size should be chosen, adopting the quality of image as the basic criterion (a compromise between resolution and image blur), which is particularly important in the case of a small number M of rays (Fig. 9).

7. Experimental verification

To verify the reconstruction performance of the convolution and backprojection algorithm optimized in this research, actual measurements were made using a UTT experimental setup [3]. To measure transition time, a computer flaw detector card with a resolution of 14 ns (this resolution is determined by card's sampling rate — 72 MHz) and a pair of ultrasonic transducers: a sending one and a receiving one, operating at frequency of 2.5 MHz, were used. A quasi-homogenous cylinder 50 mm in diameter and 70 mm high, formed from agar gel and immersed in water, was measured. The sound velocity in the cylinder was about 1505 m/s and in water — 1491 m/s. A measuring area whose diameter was equal to the sending transducer–receiving transducer distance $l_o = 100$ mm was assumed. A set of measuring data — mean times of passage through the circular cross-section of the cylinder — in a parallel ray projection geometry was obtained (Fig. 1) for $M = 101$ rays and $N = 100$ projections. The obtained data were recalculated to mean noise velocities for the distance of 100 mm and, after reduction and re-scaling according to method B (Sec. 4), they were entered into the convolution and backprojection algorithm in order to reconstruct an image of the distribution of local sound velocities in the investigated cylinder cross-section. During reconstruction 6 different values of parameter E for applied convolving function q (formula (11)): 0, 0.2, 0.4, 0.6, 0.8, 1 were assumed in turn. The data obtained immediately after reconstruction were recalculated to sound velocity using formula (19) and imaged in a 16-degree gray scale (Fig. 10) and in pseudo-3D (Fig. 11).

The cylinder cross-section images reconstructed on the basis of the actual measurements (Figs. 10 and 11) are very similar to images reconstructed from simulations (Fig. 4). This shows that the optimized convolution and backprojection algorithm operation is correct. The oscillations of sound velocities in the images (Figs. 10, 11) are caused by the agar gel heterogeneity.

For low values of parameter E of convolving function q (formula (11)) one can obtain sharp images with clearly visible edges along discontinuities (Figs. 10 a, b, c and 11 a, b, c). A shortcoming of this kind of reconstruction are oscillations of the reconstructed values close to all, even small, discontinuities.

For high values of parameter E reconstructed images are less contrasty — the boundaries of non-homogenous structures are blurred and the small discontinuities are not visible (Figs. 10 d, e, f and 11 d, e, f). But the advantage of such reconstructions is that there are no oscillations or interference which in the case of the visualization of slightly heterogeneous structures may falsify the image.

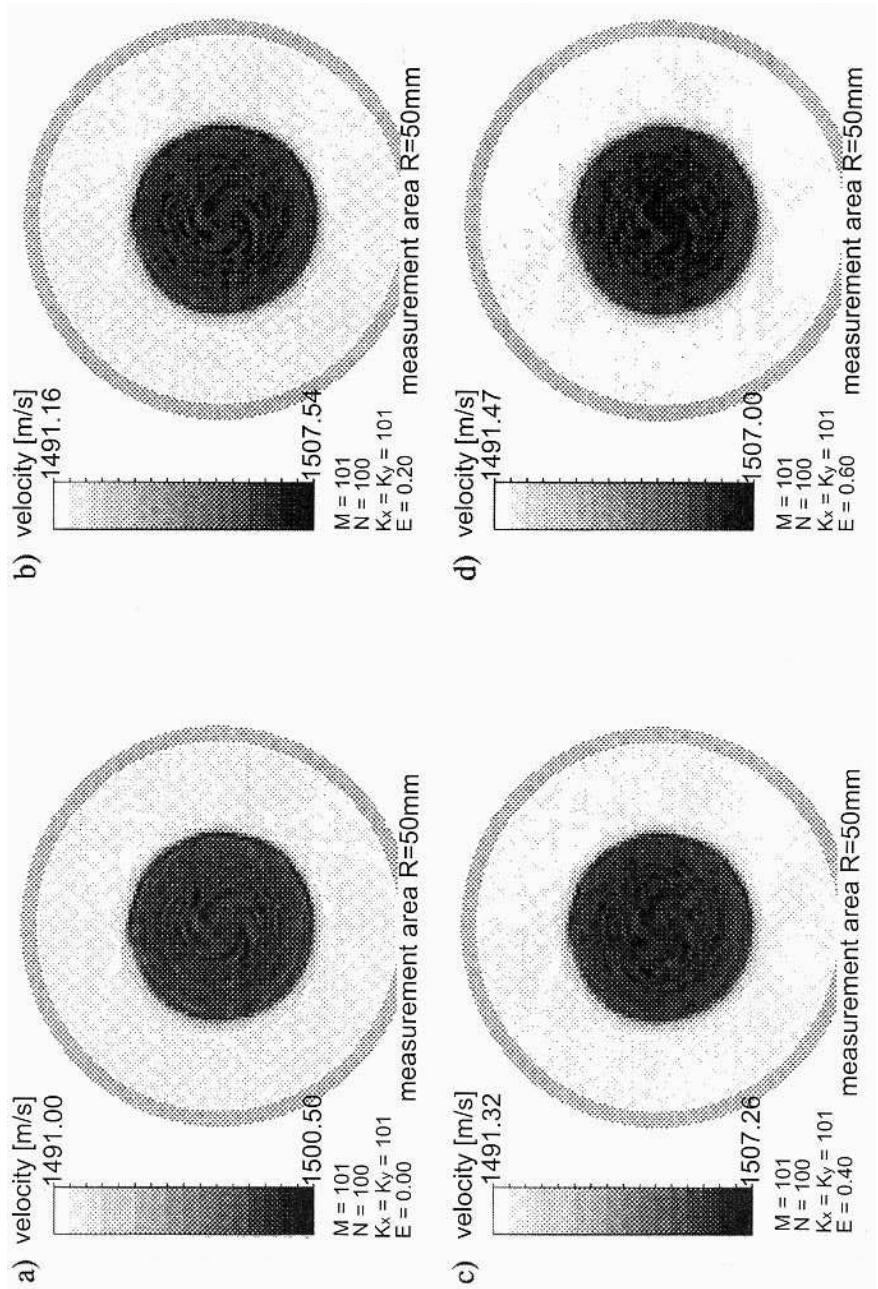
a) velocity [m/s]
1491.00
1500.50
M = 101
N = 100
Kx = Ky = 101
E = 0.00
measurement area R=50mm
b) velocity [m/s]
1491.16
1507.54
M = 101
N = 100
Kx = Ky = 101
E = 0.20
measurement area R=50mm
c) velocity [m/s]
1491.32
1507.26
M = 101
N = 100
Kx = Ky = 101
E = 0.40
measurement area R=50mm
d) velocity [m/s]
1491.47
1507.00
M = 101
N = 100
Kx = Ky = 101
E = 0.60
measurement area R=50mm

[Fig. 10]

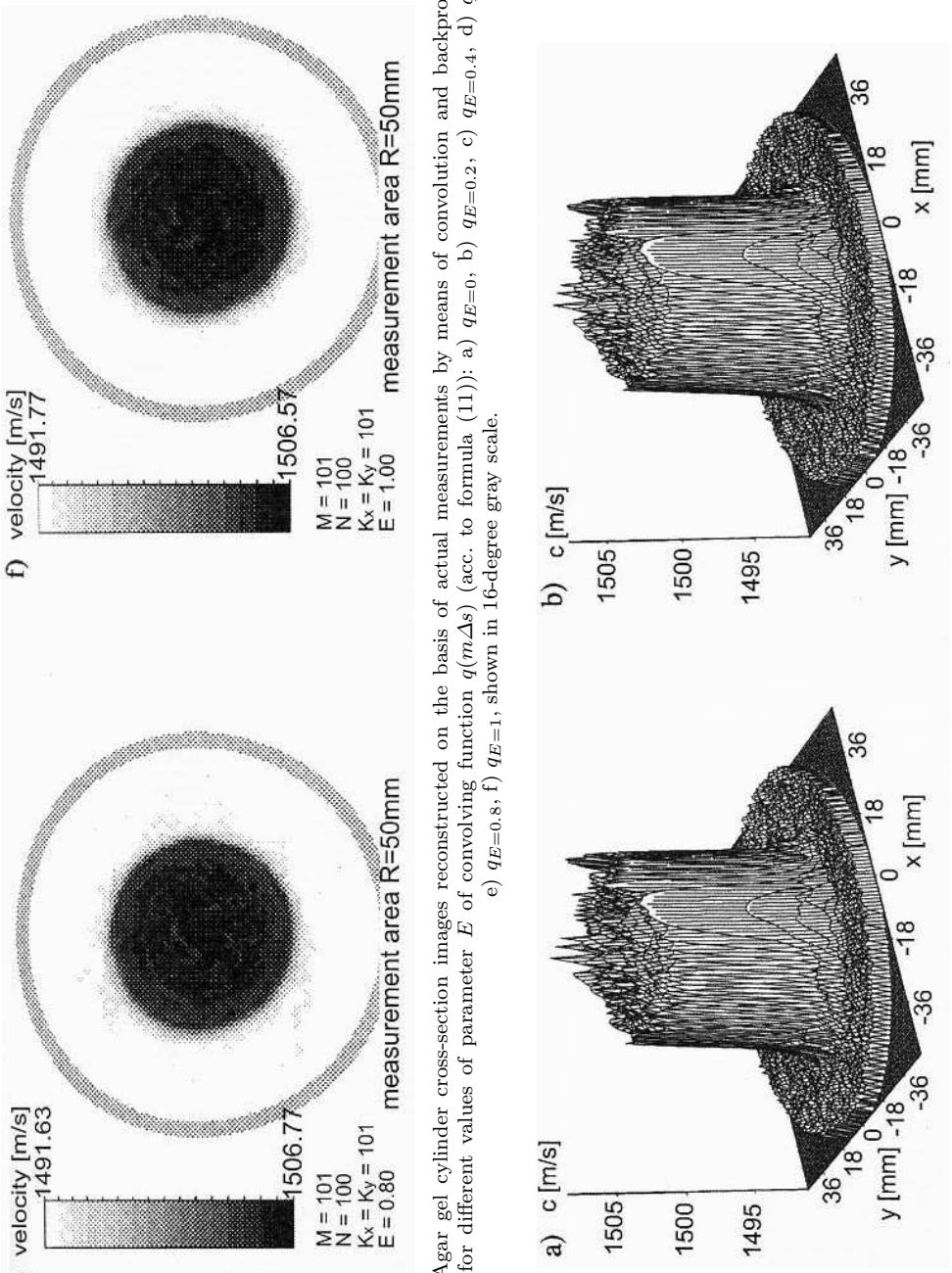

Fig. 10. Agar gel cylinder cross-section images reconstructed on the basis of actual measurements by means of convolution and backprojection algorithm for different values of parameter E of convolving function $q(m\Delta s)$ (acc. to formula (11)): a) $q_{E=0}$, b) $q_{E=0.2}$, c) $q_{E=0.4}$, d) $q_{E=0.6}$, e) $q_{E=0.8}$, f) $q_{E=1}$, shown in 16-degree gray scale.

[Fig. 11]

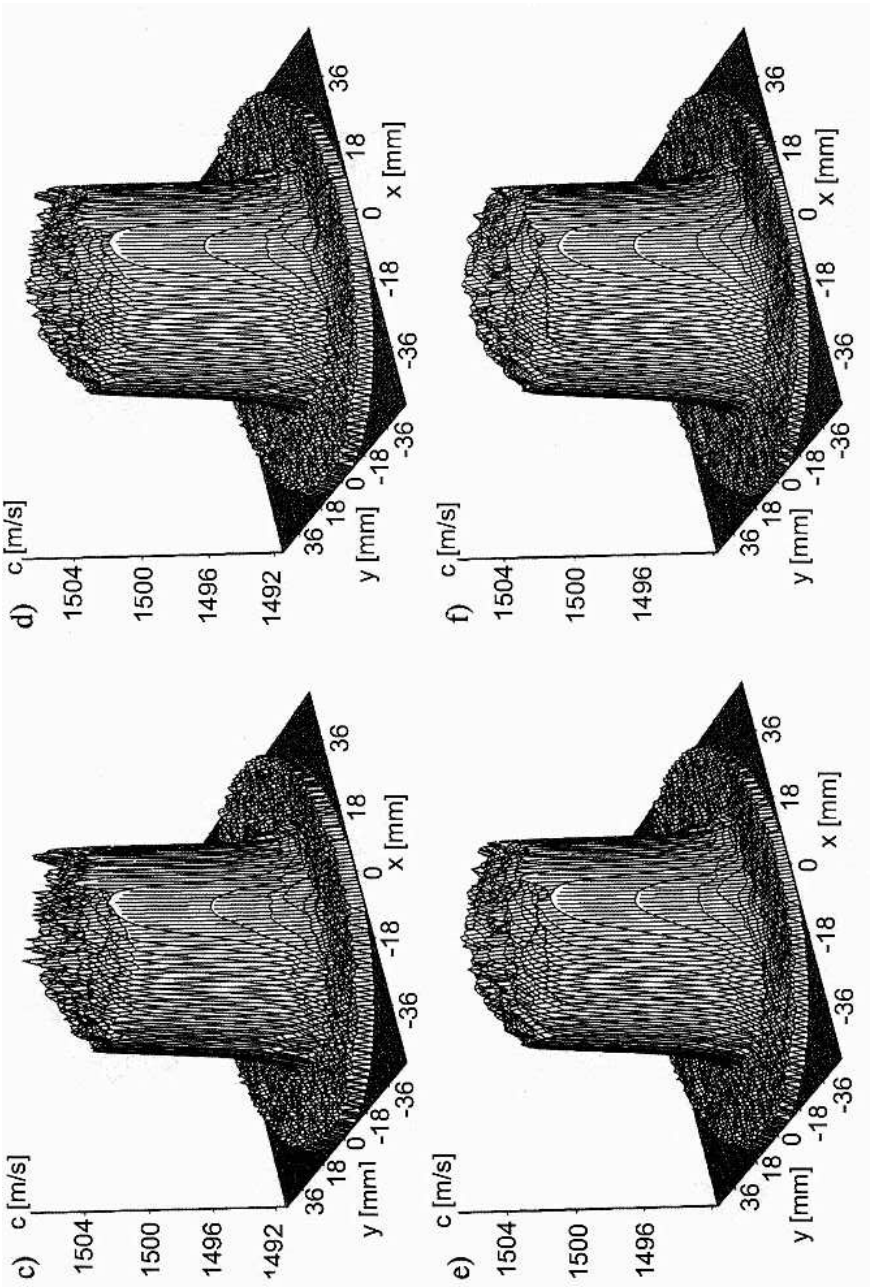

Fig. 11. Agar gel cylinder cross-section images reconstructed on the basis of actual measurements by means of convolution and backprojection algorithm for different values of parameter E of convolving function $q(m\Delta s)$ (acc. to formula (11)): a) $q_{E=0}$, b) $q_{E=0.2}$, c) $q_{E=0.4}$, d) $q_{E=0.6}$, e) $q_{E=0.8}$, f) $q_{E=1}$, shown in pseudo-3D.

8. Conclusions

After appropriate optimization, the convolution and backprojection algorithm is perfectly suitable for UTT purposes because of its application versatility and the compromise between the imaging accuracy and the computation time. The use of convolving function $q(m \cdot \Delta s)$ (formula (11)), presented in paper [6] by R.M. Lewitt, in this algorithm ensures that in UTT it is possible to reconstruct the object internal structure images of different contrast by controlling the value of parameter E within range $[0, 1]$ without the necessity of introducing other convolving functions.

The convolution and backprojection algorithm presented and optimized in this research can be applied directly to the UTT visualization of an object's internal structure as the distribution of local sound velocities in it, reconstructed on the basis of the mean times of passage of an ultrasonic wave through the object immersed in water, in a parallel ray projection geometry.

The method of fitting proposed here, scaling and correcting transition time measuring data before they are entered into the reconstruction algorithm, makes it possible to obtain accurate local sound velocities after the reconstruction. This method has been verified by simulation calculations and actual measurements, which have shown that quite an accurate tomographic image can be obtained already for half the number of rays which follows from the number-of-projections-to-number-of-rays criterion (formula (20)). As regards the reconstruction process itself, it is enough to satisfy this criterion to obtain good-quality tomographic images. It has been found that a cross-section of homogenous structure can be visualized by UTT with high accuracy using the convolution and backprojection algorithm, if $M \geq 51$ rays per cross-section's largest dimension and $N \geq 81$ projections are assumed and if we have error-free mean transition measurements obtained in a parallel ray projection geometry.

Number of rays M determines the resolution of an image, the accuracy with which the size of structures is imaged and the accuracy of the reconstruction of image point values. Number of projections N determines the image's dynamics and distortions: if it is too low, distortions in the form of streaks and glow, which extend the scale of reconstructed values downwards, appear.

Because of computation time and image blur, an optimum size of reconstruction grid $K \times L$ — according to the visualization criterion — should be chosen.

Acknowledgements

This research was carried out as part of grant no. 8 T11E 029 14 funded by KBN (Scientific Research Committee) in the years 1998–2000.

References

[1] Y. Censor, *Finite series-expansion reconstruction methods*, Proceedings of the IEEE, **71**, 3, 409–419 (1983).

[2] E.J. Farrell, *Processing limitations of ultrasonic image reconstruction*, Proc. of 1978 Conf. on Pattern Recognition and Image Processing (1978).

[3] T. Gudra, K. Opieliński and W. Selwesiuk, *Experimental setup for ultrasound transmission tomography* [in Polish], Proceedings of XLIII Open Seminar on Acoustics OSA'96, **1**, 259–264 (1996).

[4] A.K. Jain, *Fundamentals of digital image processing*, Prentice-Hall, Englewood Cliffs, New Jersey 1989, p. 570.

[5] A.C. Kak and M. Slaney, *Principles of computerized tomographic imaging*, The IEEE Inc., IEEE Press, New York 1988, p. 329.

[6] R.M. Lewitt, *Reconstruction algorithms: transform methods*, Proceedings of the IEEE, **71**, 3, 390–408 (1983).

[7] S.A. Nielsen, K.K. Borum and H.E. Gundtoft, *Veryfying an ultrasonic reconstruction algorithm for non-destructive tomography*, Proc. Of The 1995 World Congress on Ultrasonics, 447–450 (1995).

[8] K. Opieliński, *Computer model of ultrasound transmission tomography: reconstruction of images* [in Polish], Proceedings of XLIII Open Seminar on Acoustics OSA'96, **2**, 547–552 (1996).

[9] K. Opieliński, *Imaging of object's internal structure by ultrasound transmission tomography (UTT) on the basis of computer simulation of acoustic parameters* [in Polish], Acoustics in Technology, Medicine and Culture — KBN Grant Projects carried out in the years 1993–1995, 215–220 (1996).

[10] K. Opieliński, *Reconstruction of image of object's internal structure by ultrasound transmission tomography (UTT) on the basis of computer simulation of ultrasound velocity measurements* [in Polish], Molecular and Quantum Acoustics, **17**, 219–226 (1996).

[11] G.N. Ramachandran and A.V. Lakshminarayanan, *Three dimensional reconstructions from radiographs and electron micrographs: Application on convolution instead of Fourier transforms*, Proc. Nat. Acad. Sci., **68** (1971).

[12] L.A. Shepp and B.F. Logan, *The Fourier reconstruction of a head section*, IEEE Trans. Nucl. Sci., NS-21 (1974).

[13] M. Stapper and G. Sollie, *Ultrasound transmission tomography by means of a personal computer*, Ultrasonics International'85, 935–940 (1985).